Molecular Biology of the Cell
Vol. 17, 4343–4352, October 2006

Novel Function of Clathrin Light Chain in Promoting Endocytic Vesicle Formation[D] [V]

Thomas M. Newpher,* Fatima-Zahra Idrissi,† Maria Isabel Geli,† and Sandra K. Lemmon*

*Department of Molecular and Cellular Pharmacology, University of Miami, Miami, FL 33101; and †Instituto de Biología Molecular de Barcelona (IBMB), Consejo Superior de Investigaciones Científicas, 08034 Barcelona, Spain

Submitted July 17, 2006; Accepted July 19, 2006
Monitoring Editor: Sandra Schmid

Clathrin-mediated endocytosis is a major pathway for uptake of lipid and protein cargo at the plasma membrane. The lattices of clathrin-coated pits and vesicles are comprised of triskelions, each consisting of three oligomerized heavy chains (HC) bound by a light chain (LC). In addition to binding HC, LC interacts with members of the Hip1/R family of endocytic proteins, including the budding yeast homologue, Sla2p. Here, using in vivo analysis in yeast, we provide novel insight into the role of this interaction. We find that overexpression of LC partially restores endocytosis to cells lacking clathrin HC. This suppression is dependent on the Sla2p binding region of LC. Using live cell imaging techniques to visualize endocytic vesicle formation, we find that the N-terminal Sla2p binding region of LC promotes the progression of arrested Sla2p patches that form in the absence of HC. We propose that LC binding to Sla2p positively regulates Sla2p for efficient endocytic vesicle formation.

INTRODUCTION

Clathrin is a major vesicle coat protein that is important for receptor-mediated endocytosis and sorting of cargo at the *trans*-Golgi network (TGN) and endosomal system (reviewed in Brodsky *et al.,* 2001). Clathrin heavy chain (HC) monomers oligomerize into triskelions containing three radially extended legs, each with an associated clathrin light chain (LC). The central region of LC binds the HC proximal leg (Scarmato and Kirchhausen, 1990; Chen *et al.,* 2002), whereas the C-terminus of LC is oriented toward the HC trimerization domain (Fotin *et al.,* 2004). Studies from yeast indicate that LCs are indeed important for efficient HC trimerization (Chu *et al.,* 1996; Huang *et al.,* 1997).

LCs may also regulate the assembly of clathrin lattices, as addition of LC to free HC trimers or recombinant HC hub fragments inhibits their spontaneous assembly (Ungewickell and Ungewickell, 1991; Liu *et al.,* 1995). This effect depends on acidic residues in an N-terminal conserved region in LC (Ybe *et al.,* 1998). The same region of LC also interacts with the central coiled-coil domain of the Hip1/R family of actin-binding endocytic proteins (Chen and Brodsky, 2005; Legendre-Guillemin *et al.,* 2005). Binding of Hip1/R to clathrin LC is required for them to promote clathrin assembly in vitro (Engqvist-Goldstein *et al.,* 2001; Chen and Brodsky, 2005; Legendre-Guillemin *et al.,* 2005). Therefore, it is hypothesized that Hip1/R promote clathrin assembly by releasing LC's inhibition of lattice assembly (Chen and Brodsky, 2005; Legendre-Guillemin *et al.,* 2005). Hip1 family members also interact with phosphatidyl-inositol lipid through an N-terminal ANTH domain and F-actin through a talin-Hip1/R/Sla2p actin-tethering C-terminal homology (THATCH) domain, suggesting that these proteins also serve to coordinate the actin cytoskeleton at clathrin-coated pits (McCann and Craig, 1997; Engqvist-Goldstein *et al.,* 1999; Legendre-Guillemin *et al.,* 2002; Hyun *et al.,* 2004; Senetar *et al.,* 2004; Sun *et al.,* 2005).

In vivo studies in yeast are beginning to elucidate the relationship between clathrin and the Hip1/R homologue, Sla2p, during endocytosis. Kinetic studies of fluorescently labeled endocytic proteins have identified multiple stages of protein recruitment during vesicle internalization (Kaksonen *et al.,* 2003, 2005; Newpher *et al.,* 2005; Newpher and Lemmon, 2006; Toshima *et al.,* 2006). Initially, clathrin and Ede1p, an Eps15 homology (EH) domain protein, are recruited to the cell cortex and are later joined by Sla2p. These are then followed by other early stage endocytic factors such as the SH3 domain protein Sla1p and the EH domain factors Pan1p and End3p. In addition, cargo recruitment to endocytic patches occurs after Ede1p arrival, but before Sla1p (Toshima *et al.,* 2006). In the later stages, Abp1p, actin, and Arp2/3 complex are recruited, which coincides with membrane invagination. Finally, early stage factors uncoat and there is a rapid inward movement of the Abp1p/actin-associated endocytic vesicle into the cell.

Studies investigating the function of Sla2p during endocytic patch formation found in *sla2*Δ cells, early stage endocytic factors including clathrin, epsins, AP180s, Sla1p, Pan1p, and Las17p all accumulate in arrested cortical patches, whereas Abp1p and actin develop into comet tails that plume inward from the cortex (Kaksonen *et al.,* 2003; Newpher *et al.,* 2005). The inability of the early coat factors to

This article was published online ahead of print in *MBC in Press* (http://www.molbiolcell.org/cgi/doi/10.1091/mbc.E06–07–0606) on July 26, 2006.

[D] [V] The online version of this article contains supplemental material at *MBC Online* (http://www.molbiolcell.org).

Address correspondence to: Sandra K. Lemmon (slemmon@miami.edu).

Abbreviations used: HC, heavy chain; LC, light chain; CCV, clathrin-coated vesicle; TGN, *trans*-Golgi network; WT, wild type; GFP, green fluorescence protein; RFP, red fluorescence protein; GST, glutathione-*S*-transferase; USH, upstream alpha helix; THATCH, talin-Hip1/R/Sla2p actin-tethering C-terminal homology.

Table 1. *Saccharomyces cerevisiae* strains

Strain	Genotype
BJ3556	*MATa sst1-2 ade2-1 his6 met1 cyh2 rme1 ura1 can1*
SL1462	*MATa leu2 ura3-52 trp1 his3-Δ200*
SL1463	*MATα leu2 ura3-52 trp1 his3-Δ200*
SL1620	*MATα leu2 ura3-52 trp1 his3-Δ200 clc1Δ::HIS3*
SL2726	*MATα leu2 ura3-52 trp1 his3-Δ200 chc1-ts*
SL3593	*MATa leu2 ura3-52 trp1 bar1–1 chc1Δ::LEU2*
SL4782	*MATa leu2 ura3 his3-Δ200 trp1 clc1Δ::KanMX6 sla2Δ::LEU2* p111-Sla2-GFP [*CEN, LEU2, SLA2-GFP:TRP1*]
SL4838	*MATα leu2 ura3-52 trp1 his3-Δ200 clc1Δ::HIS3 chc1Δ::LEU2* pTMN37 [*CEN, URA3, GFP-CLC1*]
SL4896	*MATa leu2 ura3 his3-Δ200 trp1 chc1Δ::LEU2 sla2Δ::LEU2* p111-Sla2-GFP [*CEN, LEU2, SLA2-GFP:TRP1*]
SL5185	*MATα leu2 ura3 trp1 his3-Δ200 sla2Δ::LEU2 ABP1-mRFP:KanMX6* p111-Sla2-GFP [*CEN, LEU2, TRP1, SLA2-GFP*]
SL5226	*MATα leu2 ura3 his3-Δ200 trp1 chc1Δ:LEU2 sla2Δ::LEU2 ABP1-mRFP:KanMX6* p111-Sla2-GFP [*CEN, LEU2, SLA2-GFP:TRP1*]
SL5239	*MATα leu2 ura3 his3-Δ200 trp1 clc1Δ::HIS3 sla2Δ::LEU2 ABP1-mRFP:KanMX6* p111-Sla2-GFP [*CEN, LEU2, SLA2-GFP:TRP1*]

progress into the mobile actin-dependent stage suggests that one important role for Sla2p may be to couple the actin polymerization machinery with the vesicle coat. In addition, these data demonstrate that Sla2p is not necessary to promote clathrin assembly at endocytic sites in vivo (Newpher *et al.*, 2005). Conversely, we have shown that clathrin is important for progression of Sla2p containing endocytic patches. Clathrin mutants have normal numbers of endocytic patches containing Sla2p, but many never internalize or they have abnormally long lifetimes before progression to the actin driven invagination stage, and they periodically produce actin comet tails (Newpher and Lemmon, 2006). Furthermore, for arrested Sla2p patches that do ultimately internalize, there is a dramatic delay in recruitment of other early endocytic factors (e.g., Sla1p), and the actin phase is slowed. These defects suggest that clathrin has an organizational role in forming endocytic sites and/or it promotes the progression of Sla2p-containing early patches.

In this article we investigate the role of LC in progression of Sla2p patches. Our previous work showed that yeast LC interacts with the Sla2p coiled-coil domain, like its mammalian counterparts (Henry *et al.*, 2002, Newpher and Lemmon, 2006). Here we gain new insight into the role of this interaction. We find that binding of the N-terminal domain of LC to Sla2p promotes progression of early endocytic structures to the invagination stage of vesicle internalization.

METHODS AND MATERIALS

Strains and Growth Assays

Strains used in this study are listed in Table 1. YEPD and synthetic dropout medium were prepared as described in Newpher and Lemmon (2006). Cells were usually cultured at 30°C. For the growth assay in Figure 3, cells were diluted to 10^7 cells/ml, spotted on YEPD, and grown for three d at 30°C or 37°C. In Figure 5, cells were grown overnight and serial fourfold dilutions starting at 10^7 cells/ml were spotted on YEPD plates and grown for 2 d at 30°C or 37°C.

Plasmids

Plasmids pTMN17 (*GFP-CLC1*, *TRP1*, *CEN*) and pTMN37 (*GFP-CLC1*, *URA3*, *CEN*) are described in Newpher *et al.* (2005). YCp50-*CHC1* was described in Lemmon and Jones (1987). YEp24-*CHC1*, pKH4 (*CLC1*, *URA3*, *CEN*), and pKH2 (*CLC1*, *URA3*, *2μ*) were previously described in Huang *et al.* (1997). p111-*SLA2-GFP* (*CEN*, *TRP1*, *LEU2*) was described in Newpher and Lemmon (2006). Plasmids pTMN1 (GST-*CLC1* for bacterial expression), pTMN3 (6xHis-*CLC1* for bacterial expression), pTMN10 (6xHis-*clc1-[77-233]*), pTMN11 (6xHis-*clc1-[77-155]*), pTMN12 (6xHis-*clc1-[1–155]*), pTMN14 (6xHis-*clc1-[41-233]*), pTMN15 (6xHis-*clc1-[19-233]*) were constructed by amplifying with *CLC1* primers and subcloning into pGEX-2T (Amersham Biosciences, Piscataway, NJ) or pRSET-A (Invitrogen, Carlsbad, CA), using BamHI/EcoRI restriction sites. pTMN16 (GST-*chc1-[1062-1653]*) was constructed by amplifying *CHC1* coding sequence with primers containing flanking NotI and SalI restriction sites for subcloning into pGEX-4T1 (Amersham Biosciences). pTMN18 (*CEN*, *TRP1*, *clc1-[77-233]*), pTMN19 (*CEN*, *TRP1*, *clc1-[41-233]*), and pTMN20 (*CEN*, *TRP1*, *clc1-[1-143]*) were made in a two-step process. First *His3MX6* with flanking NcoI sites was amplified from pFA6a-His3MX6 (Longtine *et al.*, 1998) with *CLC1* primers containing sequence flanking the truncation or internal deletion sequences and gap repaired into pKH1 (*CEN*, *TRP1*, *CLC1*) or pRS424-*CLC1* (*2μ*, *TRP1*, *CLC1*). Plasmids from His^+ Trp^+ transformants were digested with NcoI to remove the *His3MX6* cassette and self-ligated to generate the above truncation and deletion mutants. pTMN27 (*2μ*, *URA3*, *clc1-[77-233]*), pTMN28 (*2μ*, *URA3*, *clc1-[1-143]*), and pTMN29 (*2μ*, *URA3*, *clc1-[41-233]*) were generated by PvuII digestion of pTMN18, pTMN20, and pTMN19, respectively, and gap repairing into BamHI-cut pRS426 (*2μ*, *URA3*). pTMN42 was made by integrating the *His3MX6* cassette flanked by NcoI sites directly after the *CLC1* start codon of pKH1. The *His3MX6* cassette was removed by digestion with NcoI and religation. pTMN44 (*CEN*, *TRP1*, *GFP-clc1[-77-233]*) was made by PCR amplifying the GFP-coding sequence from pFA6a-GFP(S65T)-TRP1 (Longtine *et al.*, 1998) with ends upstream of the *CLC1* start codon and downstream of the truncation sequence and gap repairing into NcoI-cut pTMN42. pTMN48 (*CEN*, *TRP1*, *GFP-clc1-[1-143:HIS3Mx6]*) was made by integrating a stop codon into pTMN17 (*CEN*, *TRP1*, *GFP-CLC1*) after codon 143 using the *His3MX6* cassette amplified from pFA6a-His3MX6. GST-*sla2*–289-583 was described in Newpher and Lemmon (2006). GST-*BMH1*, was a generous gift from Mike Yaffe. All plasmids generated by PCR of coding sequences were verified by DNA sequencing.

Biochemical Procedures

GST and 6xHis fusion proteins were purified and pulldown experiments were performed as described in Newpher and Lemmon (2006).

Clathrin-coated vesicles were purified from yeast as described in Lemmon *et al.* (1988). Fractions from Sephacryl S-1000 chromatography were analyzed by SDS-PAGE and immunoblotted with mouse monoclonal antibodies against clathrin HC (Lemmon *et al.*, 1988).

For immunoblots of clathrin LC, extracts were prepared by glass bead lysis with 2.0×10^8 cells in 1 ml of 150 mM NaCl, 1.0% NP-40, 0.5% deoxycholate, 0.1% SDS, 50 mM Tris (pH 8.0). Extracts were spun at $10{,}000 \times g$ for 10 min to remove debris, boiled for 5 min, analyzed by SDS-PAGE, and immunoblotting with rabbit anti-Clc1p antibodies at 1:1000 (gift from Greg Payne).

Alpha-Factor Uptake Assay

For endocytosis assays, ^{35}S-labeled α-factor uptake was monitored at 25°C essentially as described in Dulic *et al.* (1991) using the continuous presence protocol assay. Radioactive α-factor was purified using a CG-50 column. Background binding was determined from an assay performed in the presence of 40 μM cold α-factor and was subtracted from each sample. Plots show best-fit trend lines generated in Microsoft Excel (Redmond, WA). Data are the average of four independent experiments ± SD.

Microscopy

Fluorescent fusion proteins were visualized in live cells by growing cultures overnight to midlog phase in synthetic media. Time-lapse videos were collected from cells immobilized in 0.8% low-melt agarose prepared in complete synthetic medium. Microscopy was performed using an Olympus fluorescence BX61 microscope (Melville, NY) equipped with Nomarski differential interference contrast (DIC) optics, a 100× objective (NA 1.35), a Roper CoolSNAP HQ camera (Tucson, AZ), Sutter Lambda 10 + 2 automated excitation and emission filter wheels (Novato, CA) and a 175 W Xenon remote source lamp with liquid light guide. Images were acquired and processed using the Intelligent Imaging Innovations (Denver, CO) SlideBook image analysis software and prepared with Adobe Photoshop 7 (San Jose, CA). Time-lapse video composites were generated using ImageJ software (http://rsb.info.nig.gov/ij/). Kymographs were generated from single-pixel-wide lines taken during 4-min time-lapse videos. Exposure times of 500 ms were used for all wide-field images. Patch lifetimes of Sla2p and Abp1p are displayed as the mean ± the SD in seconds.

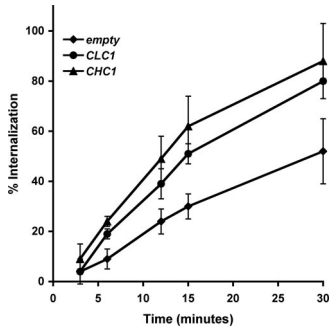

Figure 1. LC overexpression suppresses the α-factor internalization defect of *chc1*Δ cells. *MAT***a** *chc1*Δ *bar1-1* (SL3593) was transformed with YEp24-*CHC1* (*CHC1*, 2μ), pKH2 (*CLC1*, 2μ), or pRS426 (empty 2μ). α-factor uptake was analyzed as described in *Materials and Methods*.

RESULTS

Overexpression of LC Partially Suppresses the Endocytic Defect of Clathrin HC-deficient Cells

Previously we identified the clathrin LC gene, *CLC1*, as a multicopy suppressor of the growth defects of clathrin HC–deficient yeast (Nelson and Lemmon, 1993; Huang *et al.*, 1997). Although LC overexpression suppressed growth, it did not suppress the TGN sorting defects of *chc1*Δ cells (Huang *et al.*, 1997). It has since remained a mystery how the clathrin LC could function in the complete absence of HC. Because yeast LC, like its mammalian counterparts, interacts directly with the Sla2p coiled-coil domain (Newpher and Lemmon, 2006), we tested whether LC was suppressing the endocytic phenotype of clathrin-deficient yeast. We found that LC overexpression partially suppressed the α-factor internalization defect of *chc1*Δ cells (Figure 1).

N-Terminus of LC Binds Sla2p and Partially Suppresses the Growth and Endocytic Defects of Clathrin HC–deficient Cells

To determine if the Sla2p-binding region is responsible for LC suppression of *chc1*Δ endocytic defects, GST pulldowns using bacterially expressed protein were performed to map the regions of yeast LC that bind Sla2p and HC. 6xHis-tagged N- and C-terminal deletion constructs of Clc1p were first incubated with GST fused to the HC proximal region (GST-Chc1p-[1062-1653], Figure 2, A and B). Deletion of the first 18 (Clclp-[19-233]), 40 (Clc1p-[41-233]), or 76 (Clc1p-[77-233]) residues of LC did not prevent the interaction with the clathrin HC proximal domain (GST-Chc1p-[1062-1653]); however, deletion of the last 78 residues of Clc1p (Clc1p-[77-155] or Clc1p-[1-155]), which removes most of the postulated C-terminal HC-binding region, prevented HC interaction (Figure 2, A and B).

The same 6xHis-tagged Clc1p truncations were tested for binding to GST-Sla2p-[289-583], which contains the Sla2p coiled-coil domain, previously shown to bind full-length LC (Newpher and Lemmon, 2006), like its mammalian counterparts (Legendre-Guillemin *et al.*, 2002). The first 18 residues of Clc1p were not required for Sla2p binding; however,

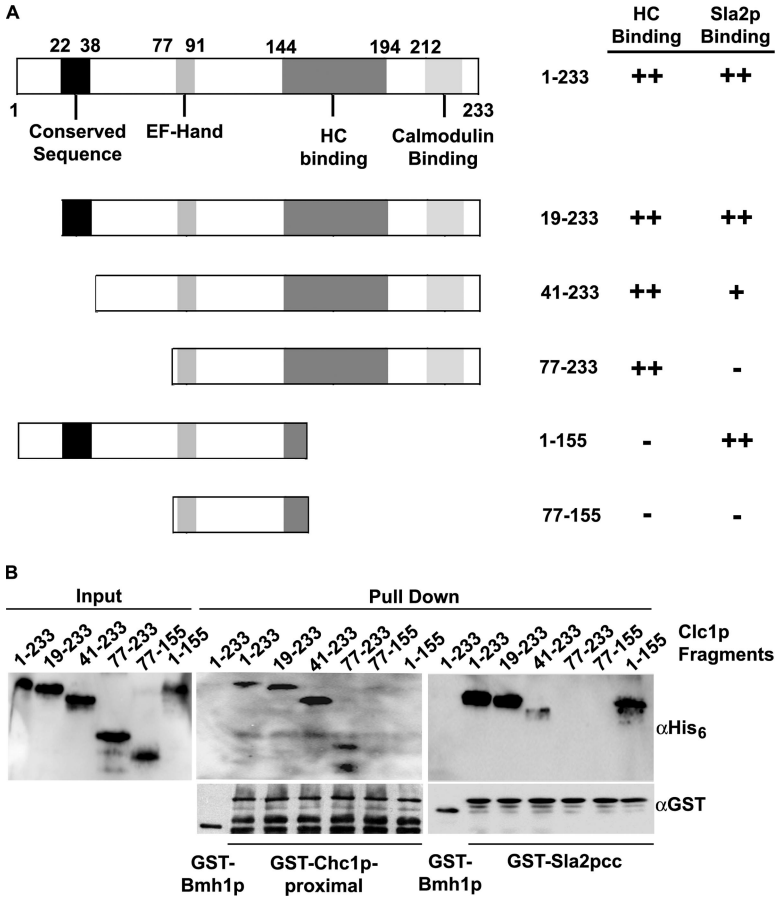

Figure 2. The N-terminus of LC (residues 19–76) interacts directly with the Sla2p coiled-coil domain. (A) 6xHis-Clc1p truncation mutants used for pulldown experiments and summary of interactions with HC or Sla2p. LC contains an N-terminal conserved sequence (22–38), a calcium-binding EF-Hand motif (80–91), an HC-binding region (144–194), and a calmodulin-binding site (212–225). (B) 6xHis tagged Clc1p truncations were used in pulldowns with GST-Chc1p-proximal leg residues [1062–1653] (middle panel) and GST-Sla2p-cc residues [289–583] (right panel) and immunoblotted with the indicated primary antibodies. The left panel shows input of 6xHis-Clc1p constructs.

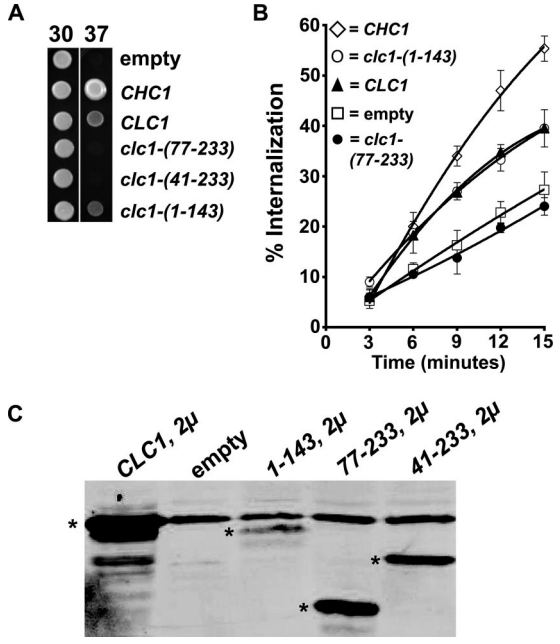

Figure 3. The Sla2p-binding region of LC suppresses growth and endocytic phenotypes of HC-deficient cells. (A) Growth of *chc1* strain (SL2726) transformed with pRS426 (empty, 2μ), YCp50-*CHC1* (*CHC1*, *CEN*), pKH2 (*CLC1*, 2μ), pTMN27 (*clc1-[77-233]*, 2μ), pTMN29 (*clc1-[41-233]*, 2μ), or pTMN28 (*clc1-[1-143]*, 2μ). (B) Endocytosis. *MAT***a** *chc1*Δ *bar1–1* (SL3593) was transformed with YEp24-*CHC1* (*CHC1*, 2μ), pTMN28 (*clc1-[1-143]*, 2μ), pKH2 (*CLC1*, 2μ), pRS426 (empty 2μ), or pTMN27 (*clc1-[77-233]*, 2μ). α-factor uptake was analyzed as described in *Materials and Methods.* (C) Immunoblot of extracts from *chc1* (SL2726) transformed with pKH2 (*CLC1*, 2μ), pRS316 (empty, *CEN*), pTMN28 (*clc1-[1-143]*, 2μ), pTMN27 (*clc1-[77-233]*, 2μ), or pTMN29 (*clc1-[41-233]*, 2μ) detected with anti-Clc1p antibodies. Asterisk indicates the band corresponding to plasmid-encoded LC fragments. Note the aberrant mobility of the LC (1–143) fragment.

deletion of the first 40 residues of Clc1p strongly reduced the interaction, whereas deletion of amino acids 1–76 completely eliminated binding (Figure 2, A and B). Importantly, Clc1p-[1-155] maintained its interaction with Sla2p, showing that the N-terminus of LC is necessary and sufficient for Sla2p interaction. These results demonstrate that the region involved in Sla2p interaction is within amino acids 19–76 of Clc1p (Figure 2A), which are separate from the HC-binding region of LC.

We next tested the requirement of Sla2p-LC interaction for LC-mediated suppression of *chc1* growth and endocytic defects. Similar to full-length LC, an N-terminal domain fragment of LC [1-143], which does not bind to HC, also partially suppressed the growth defect of *chc1* cells (Figure 3A). However, the LC alleles that remove all or portions of the Sla2p binding site (Clc1p-[77-233] and Clc1p-[41-233]) could not rescue growth (Figure 3A), despite the higher level of expression of Clc1p-[41-233] and Clc1-[77-233] compared with Clc1p-[1-143] (Figure 3C). Removal of Sla2p binding sequences within the [1-143] fragment, (Clc1p-[1-143Δ20-76], Clc1p-[1-143Δ20-40] or Clc1p-[1-143Δ41-76]) also no longer rescued growth (T. Newpher, unpublished data).

In addition to growth suppression, the N-terminus of LC (Clc1p-[1-143]), like full-length LC, partially rescued α-factor internalization in *chc1*Δ cells, whereas similar overexpression of the C-terminal HC-binding region (Clc1p-[77-233]) (Figure 3B), which lacks the Sla2p binding site had no effect. These data demonstrate that the LC can partially function during endocytosis in the complete absence of clathrin HC, and this suppression requires the Sla2p binding region on LC, but not the HC-binding domain.

The N-Terminal Sla2p-binding Region of LC Increases the Turnover Rate of Sla2p-containing Early Endocytic Patches in Clathrin Mutants

To determine what stage of endocytosis is suppressed by LC overexpression, we followed the dynamics of Sla2p-GFP and Abp1-mRFP in *chc1*Δ cells overexpressing full-length LC or the N-terminal Sla2p-binding fragment of LC [1-143]. As shown previously (Newpher and Lemmon, 2006), clathrin mutants contain many immobile early endocytic patches labeled with Sla2p (Figure 4, C and D). Cells overexpressing Clc1p or Clc1p-[1-143] still contained different classes of Sla2p patches. However, the proportion of cells in which nearly all of the Sla2p-GFP patches were mobile increased from 38% in *chc1*Δ with empty vector (n = 173 cells) to 62% when LC was overexpressed (n = 100 cells), compared with 100% in *chc1*Δ cells complemented with *CHC1* (n = 25 cells; Figure 4C, Supplementary Movie S1). Also, the percentage of cells containing mostly immobile Sla2p patches decreased from 35% in *chc1*Δ with empty vector (Figure 4C, empty) to 5% when LC was overexpressed (Figure 4C). Similar changes were observed with the N-terminal Sla2p binding fragment of LC (n = 119) (Figure 4C and Supplementary Movie 1), but not with the HC binding region (n = 95; Figure 4C; T. Newpher, unpublished observations). When only the mobile Sla2p-GFP patches were analyzed, we found that the average turnover rate was accelerated from 40 s in *chc1*Δ (n = 41 patch events) to ~28 s in cells overexpressing Clc1p or Clc1p-[1-143] (Figure 4, A and D; note shorter patch lifetimes in kymographs, $p < 0.001$, n = 60 and 90 patch events, respectively). In contrast, overexpression of the HC-binding region alone (Clc1p-[77-233]) had no effect on Sla2p patch lifetime (n = 25 patch events; Figure 4, A and D).

In *chc1*Δ cells Abp1p-RFP patches that are recruited to mobile Sla2p patches have slowed lifetimes compared with wild type (Newpher and Lemmon, 2006). This was not significantly suppressed by overexpression of Clc1p-[1-143] (Figure 4B, $p > 0.1$, n = 30 patch events), but was suppressed by overexpression of Clc1p (Figure 4B, $p < 0.001$, n = 30 patch events). The actin comet tail defect seen in *chc1*Δ cells was present when overexpressing either LC (n = 55 cells) or its N-terminal fragment (n = 44 cells), although it was less severe with full-length LC (n = 27 cells; Figure 4, C and D, arrows). These differences may be due to the higher level of protein expression for the full-length LC compared with Clc1p-[1-143] (Figure 3C). Taken together, these data indicate that the N-terminus of clathrin LC partially suppresses the endocytic phenotype of *chc1*Δ yeast through its direct interaction with Sla2p. In addition, the suppression by LC occurs during the early stage of endocytosis by accelerating Sla2p patch lifetime and increasing the proportion of cells in which all Sla2p patches are mobile.

The N-Terminal Sla2p-binding Region of LC Partially Complements **clc1-***deficient Yeast*

We also tested the ability of Clc1p-[1-143], Clc1p-[77-233] and Clc1p-[44-233] to complement the defects of LC-deficient cells. All of the LC mutant proteins were expressed and could be detected by immunoblotting with anti-Clc1p antibodies; however, Clc1p-[41-233], Clc1p-[77-233], and Clc1p-[1-143] were only detected at near normal levels by expression from 2μ plasmids (Figure 5A). Cells expressing the less stable Clc1p-[41-233] and Clc1p-[77-233] were slightly tem-

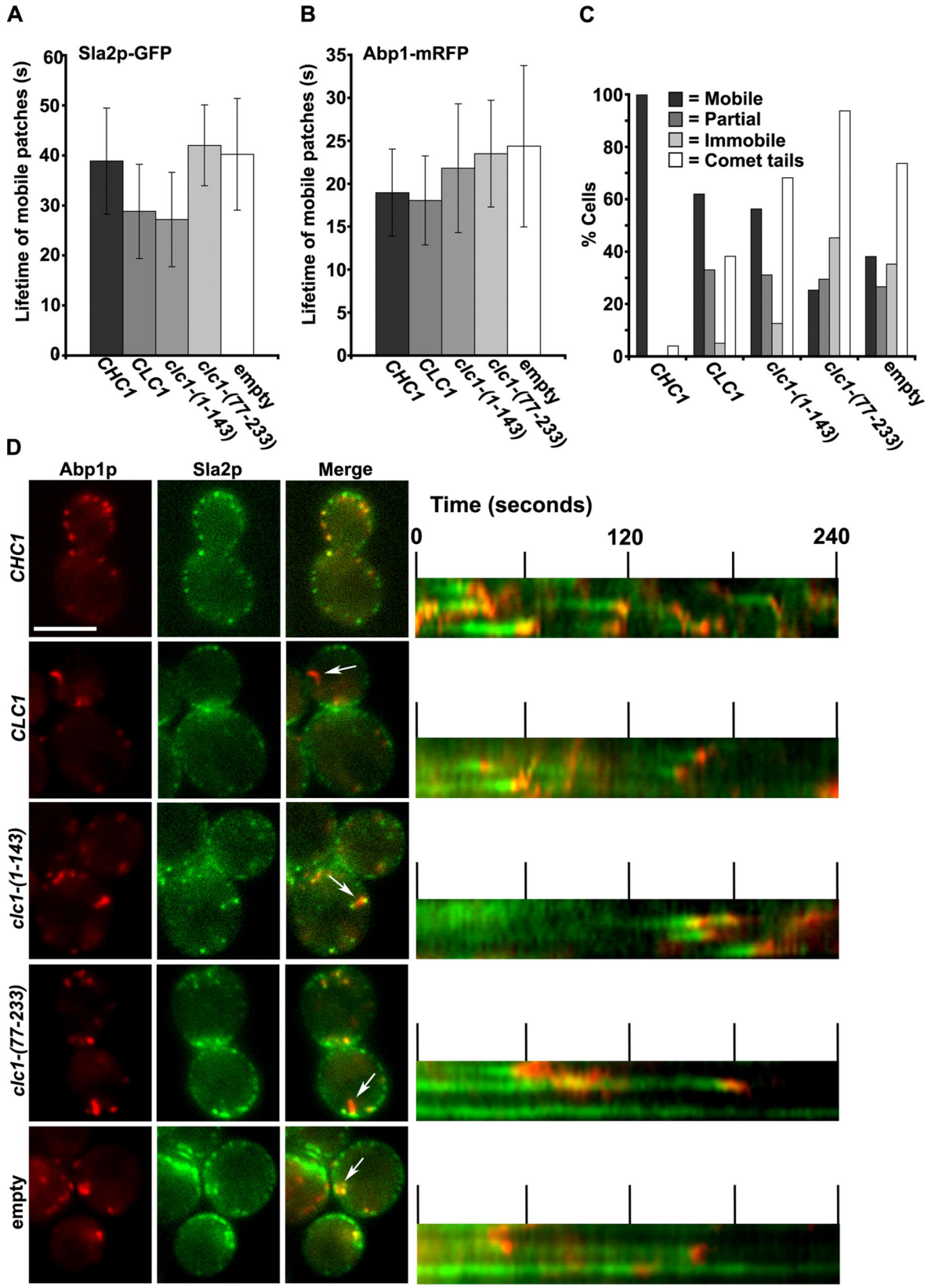

Figure 4. The Sla2p-binding region of LC increases the turnover rate of Sla2p containing early endocytic patches in *chc1*Δ. (A and B) Average lifetimes of Sla2p-GFP and Abp1p-mRFP patches in *chc1*Δ (pooled data from SL5226 and SL4896) transformed with YCp50-*CHC1* (*CHC1*, *CEN*), pKH2 (*CLC1*, 2μ), pTMN28 (*clc1-[1-143]*, 2μ), pTMN27 (*clc1-[77-233]*, 2μ), or pRS426 (empty 2μ). Images were acquired at 2-s intervals over 4 min. (C) Percentage of cells from the above strains in which nearly all Sla2p patches were mobile (Mobile), some Sla2p patches were mobile (Partial), or nearly all Sla2p patches were immobile (Immobile), and percentage of cells displaying one or more actin comet tail

perature sensitive for growth at 37°C when expressed from *CEN* plasmids (T. Newpher, unpublished observation), but showed normal WT growth at 37°C when expressed from 2μ vectors (Figure 5B). Expression of the LC N-terminal fragment (Clc1p-[1-143]) from a 2μ plasmid also partially complemented growth at 37°C and improved it at 30°C when compared with *clc1*Δ with empty vector (Figure 5B). These data indicate that that the LC N-terminal region can function independently of HC binding.

To further test the effects of impairing LC's ability to bind Sla2p or HC, *clc1-[77-233]*, *clc1-[41-233]* and *clc1-[1-143]* were assayed for their ability to rescue the TGN sorting defect of *clc1*Δ cells. Wild-type *MAT*α cells secrete the mature form of the mating pheromone α-factor, whereas clathrin mutants secrete an inactive precursor form of α-factor due to mislocalization of pro-α-factor processing enzymes, such as Kex2p, from the TGN to the cell surface (Payne and Schekman, 1989). Thus *MAT*α *clc1*Δ or *chc1*Δ cells are not competent to arrest growth of *MAT***a** cells in a halo assay (Figure 5C). The N-terminal mutants that could bind HC but not Sla2p (*clc1-[77-233]* and *clc1-[41-233]*) generated strong halos, indicating that α-factor processing and TGN sorting were restored, whereas the N-terminal fragment that could bind Sla2p but not HC (*clc1-[1-143]*) was defective (Figure 5C).

In the absence of LC, HC is not trimerized efficiently, which causes destabilization of the HC (Huang *et al.*, 1997). We found that the C-terminal HC-binding fragment [77-233], but not the N-terminal Sla2p binding domain [1-143], rescued clathrin HC steady state levels (T. Newpher, unpublished observations). Furthermore, cells expressing the C-terminal LC fragment [77-233] form clathrin-coated vesicles (CCVs), even at *CEN* level expression, whereas CCVs could not be isolated from *clc1-[1-143]* cells (Figure 5D). Therefore the N-terminal Sla2p binding region of LC (residues 1–76) is not required for TGN sorting or CCV production (Figure 5, C and D). However, the N-terminal fragment alone (Clc1p-[1-143]) is able to partially complement the temperature-sensitive growth defects of *clc1*Δ cells even without restoring TGN sorting or CCV formation.

We next tested whether Clc1p-[1-143] was able to complement the endocytic defects of *clc1*Δ yeast, by examining the dynamics of Sla2p-GFP and Abp1-RFP. Unlike *clc1*Δ with empty vector (n = 293 cells), where only 27% of the population consisted of cells in which nearly all Sla2p patches were mobile, 74% of *clc1-[1-143]* cells (n = 65 cells) exhibited mobile Sla2p patches (Figure 6, A and B; Supplementary Movie S2). Interestingly, we found that GFP-LC-[1-143] was distributed throughout the cytosol, similar to full-length GFP-LC expressed in *chc1*Δ cells, suggesting that its ability to rescue endocytosis may occur without efficient cortical patch association (Supplementary Figure 1). However, we note that in *chc1*Δ cells, 10% of LC is associated with membranes (Huang *et al.*, 1997), thus it is possible that some population of LC is present at cortical patches. We also found that 2μ expression of Clc1p-[77-233] in *clc1*Δ cells (n = 42 cells) also partially restored the percentage of cells with mobile Sla2p patches (Figure 6A). Therefore, the N-terminus of LC is not essential for endocytosis in the presence of HC, as long as the C-terminal LC region that allows trimerization

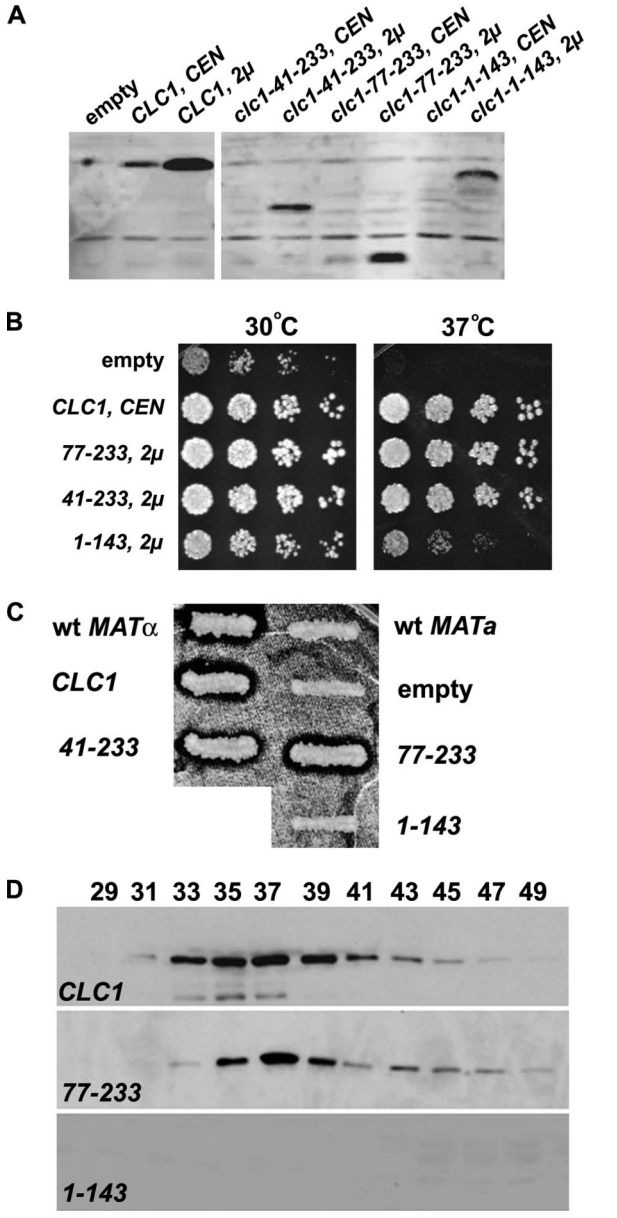

Figure 5. The N-terminus of clathrin LC complements the temperature-sensitive growth of *clc1*Δ, but not the TGN-sorting defect. (A) Immunoblot of *clc1*Δ (SL1620) transformed with pRS316 (empty, *CEN*), pKH4 (*CLC1*, *CEN*), pKH2 (*CLC1*, 2μ), pTMN26 (clc1-*[41-233]*, *CEN*), pTMN29 (*clc1-[41-233]*, 2μ), pTMN23 (*clc1-[77-233]*, *CEN*), pTMN27 (*clc1-[77-233]*, 2μ), pTMN24 (*clc1-[1-143]*, *CEN*), or pTMN28 (*clc1-[1-143]*, 2μ) detected with anti-Clc1p antibodies. (B) *clc1*Δ (SL1620) transformed with pRS316 (empty, *CEN*), pKH4 (*CLC1*, *CEN*), pTMN27 (*clc1-[77-233]*, 2μ), pTMN29 (*clc1-[41-233]*, 2μ), or pTMN28 (*clc1-[1-143]*, 2μ) were grown overnight, and serial fourfold dilutions starting at 10^7 cells/ml were spotted on YEPD plates and grown for 2 d at 30 or 37°C. (C) Halo assay of *MAT*α strains from (A) *clc1*Δ (SL1620) transformed with pKH4 (*CLC1*, *CEN*), pRS316 (empty, *CEN*), pTMN29 (*clc1-[41-233]*, 2μ), pTMN27 (*clc1-[77-233]*, 2μ), pTMN28 (*clc1-[1-143]*, 2μ), and WT controls (SL1463, *MAT*α and SL1462, *MAT***a**) patched over a *MAT***a** lawn (BJ3556). (D) Clathrin-coated vesicle preparation of WT (SL1463) and *clc1*Δ (SL1620) transformed with pTMN23 (*clc1-[77-233]*, *CEN*) or pTMN24 (*clc1-[1-143]*, *CEN*). Fractions 29–49 from the Sephacryl S-1000 column were immunoblotted with anti-Chc1p antibodies.

Figure 4 (cont). (Comet tail) in 4-min movies. (D) Left, sample images corresponding to data quantified in A–C. Note comet tails labeled with arrows. Right, kymographs of Sla2p-GFP and Abp1p-mRFP patches demonstrating the described patch behaviors in C. Also see Supplementary Movie S1. Scale bar, 5 μm.

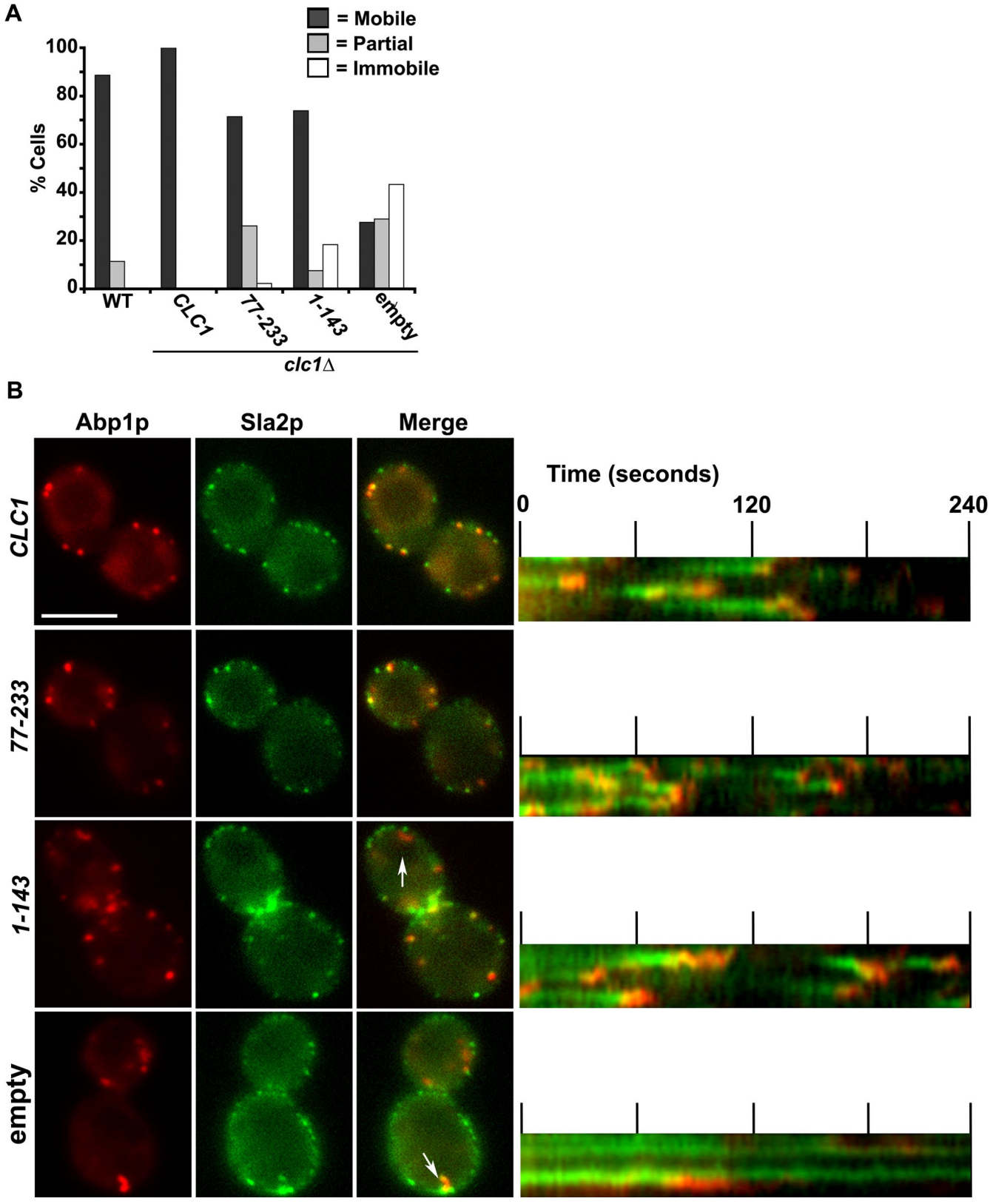

Figure 6. The Sla2p-binding region of LC increases the proportion of mobile Sla2p patches in *clc1*Δ. (A) Percentage of WT (SL5185) and *clc1*Δ (pooled data from SL5239 and SL4782) with Sla2p-GFP patch mobilities as defined in Figure 4C. *clc1*Δ cells were transformed with pKH4 (*CLC1*, *CEN*), pTMN27 (*clc1-[77-233]*, 2μ), pTMN28 (*clc1-[1-143]*, 2μ), or pRS316 (empty, *CEN*). (B) Left, sample images corresponding to data quantified in A. Right, kymographs of Sla2p-GFP and Abp1p-mRFP patches demonstrating the described patch behaviors in A. Arrows indicate examples of actin comet tails. Also see Supplementary Movie S2. Scale bar, 5 μm.

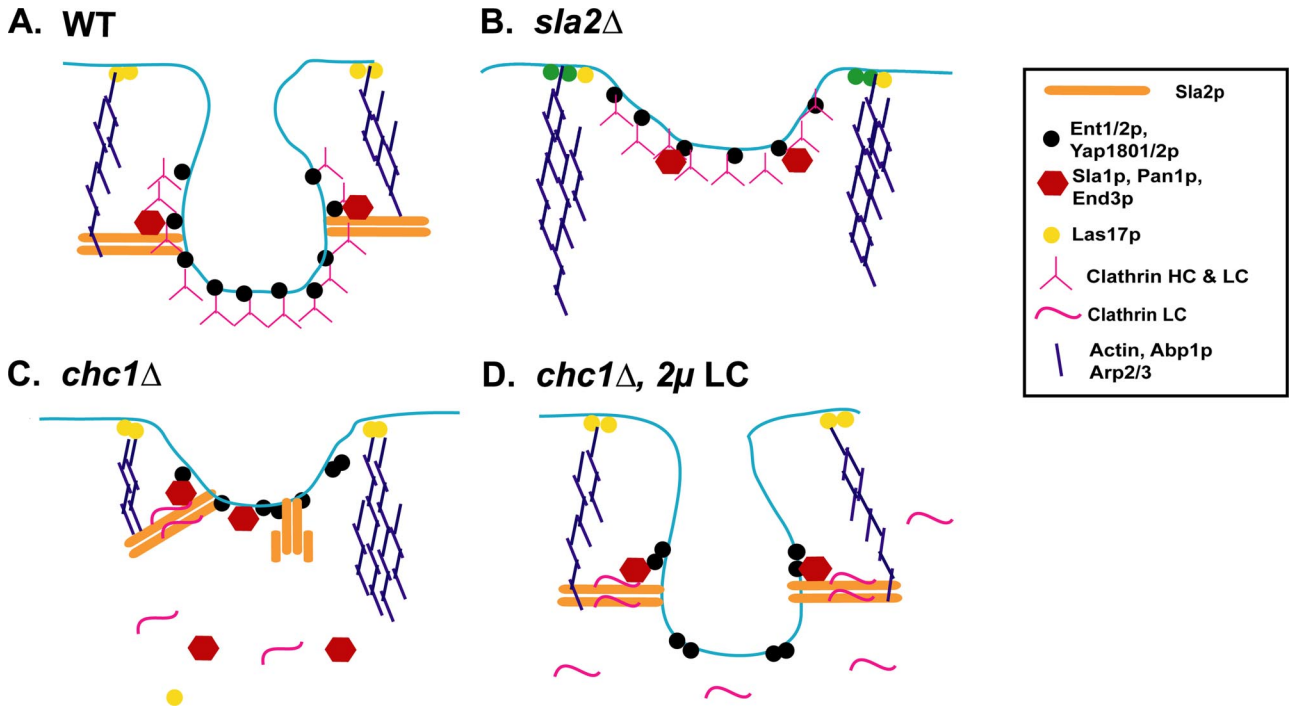

Figure 7. Model for LC activation of Sla2p during endocytosis. See *Discussion* for details.

of HC is present. This indicates that there are redundant functions provided by HCs, which may form a scaffold for recruitment of other Sla2p interacting factors at the cortex.

DISCUSSION

In this study we show that the N-terminus of yeast clathrin LC directly interacts with the coiled-coil domain of Sla2p. Like the interactions observed between mammalian LCs and Hip1/R (Legendre-Guillemin *et al.*, 2002; Chen and Brodsky, 2005), our mapping experiments implicate the LC N-terminal conserved sequence (residue 22–38) as most critical to Sla2p binding, although yeast LC sequences downstream (up to residue 76) contribute. In addition to Hip1/R binding, the acidic residues in the N-terminal conserved sequence of mammalian LC are important for LC's ability to prevent spontaneous lattice assembly in vitro (Ybe *et al.*, 1998). Furthermore, Hip1/R binding to these residues is thought to release LC's inhibition on HC and thereby promote lattice formation (Chen and Brodsky, 2005; Legendre-Guillemin *et al.*, 2005). Our studies here using in vivo analysis in yeast suggest a novel function for the LC/Sla2p interaction. Previously we identified clathrin LC as a multicopy suppressor of clathrin HC deficiency (*SCD4*; Nelson and Lemmon, 1993; Huang *et al.*, 1997). These studies demonstrated that in the complete absence of clathrin HC, the LC was capable of restoring growth, potentially through other unknown interactions. A two-hybrid screen we performed with LC as a prey only identified two interacting partners, clathrin HC and Sla2p (Henry *et al.*, 2002). Further studies confirmed Sla2p/LC binding is direct (Newpher and Lemmon, 2006). Here we have shown that the Sla2p binding region on LC is required for its ability to suppress clathrin HC deficiency. In addition, this suppression is specific for endocytosis, as LC overexpression does not rescue the TGN sorting defects of HC-deficient yeast (Huang *et al.*, 1997).

Normally we presume the LC would be present at endocytic sites in association with HC. Although we found that the N-terminal region of the LC is dispensable when HC is present, we presume that the redundancy of other contributing factors and interactions at endocytic sites, such as those mediated by the scaffolding function of clathrin, account for this. A challenge of the endocytic field has been to dissect the roles of individual protein–protein or protein–lipid interactions in the endocytic network. Thus our work demonstrates the value of in vivo analysis in a genetic system where the complexities and redundancy of the endocytic process can be investigated.

How might LC suppress the endocytic defect of *chc1*Δ cells? Because the Sla2p-binding region of LC is responsible for its suppressor activity, we measured the lifetimes of Sla2p patches during the early stage of endocytosis. Interestingly, *chc1*Δ yeast overexpressing Clc1p or Clc1p-[1-143] increased the turnover rate of mobile Sla2p-GFP cortical patches from 40 s in *chc1*Δ to ~28 s and increased the percentage of cells in which nearly all of the Sla2p patches are mobile. Therefore, LC drives or accelerates the Sla2p stage of endocytosis, likely through binding Sla2p, which ultimately increases the overall rate of endocytosis.

If LC binding to Sla2p promotes endocytic progression, what then is the function of Sla2p during endocytosis? Our results support the model where Sla2p serves as an anchor to couple the vesicle coat/early endocytic factors to the actin polymerization machinery, which ultimately provides the force for vesicle internalization (Figure 7; see Kaksonen *et al.*, 2006). Actin polymerization for endocytosis is initiated at the plasma membrane via Arp2/3 complex activators such as Las17p (Kaksonen *et al.*, 2003, 2005). To generate force for invagination of the membrane, the actin filaments would need to be tethered to the forming vesicle or associated endocytic factors. This might be mediated through an interaction with the THATCH domain of Sla2p, which would

already be recruited to the endocytic patch through its interactions with phosphatidyl-inositol lipid (via the ANTH domain), and potentially other early endocytic coat/patch factors. As actin polymerization continued at the cell surface, the force generated toward the Sla2p anchor would push the invaginating vesicle into the cell (Figure 7A). This function is consistent with the phenotypes of *sla2*Δ yeast, where the early endocytic factors are recruited but fail to internalize and actin comet tails emanating from arrested patches at the cell surface wave into the cytosol (Figure 7B), presumably unable to make productive contacts with the coat proteins (Kaksonen *et al.*, 2003; Newpher *et al.*, 2005). In addition, removal of the Sla2p talin-like domain also causes endocytic defects, demonstrating that actin binding is important for Sla2p endocytic function (Baggett *et al.*, 2003).

The interaction between LC and Sla2p could control Sla2p's ability to anchor the vesicle coat to the polymerization of actin. Previously Yang *et al.* (1999) observed an intramolecular interaction between the THATCH domain and Sla2p residues 575–767, which masks the actin-binding capabilities of Sla2p. McCann and colleagues also demonstrated with Hip1 and Hip12 (human Hip1R) that an upstream alpha helix (USH) of the THATCH domain self interacts with downstream sequences and prevents the interaction with actin (Senetar *et al.*, 2004). It is possible that binding of clathrin LC (and/or other factors to the Sla2p coiled-coil domain) could release the autoinhibition and permit THATCH domain interaction with actin, thus driving actin-based vesicle internalization. The absence of clathrin HC and its organizational functions at the early patch, would lead to loss of LC and other Sla2p binding factors (e.g., Sla1p) from cortical patches to the cytosol and favor THATCH-USH self-association (Figure 7C). Overexpression of LC, even in the absence of HC, would increase the chances of the Sla2p-LC interaction, thus suppressing the delayed endocytosis seen in *chc1*Δ (Figure 7D).

Although this model is intriguing, the region of LC binding to Sla2p is upstream of the USH, so one would have to hypothesize that LC generates a conformation change distal from its binding site. Thus far we have not observed LC interaction outside the coiled-coil domain (Newpher and Lemmon, 2006), but other sequences in LC could have a low affinity interaction that extend over into the THATCH-USH regions to mediate these effects. An alternative idea is that LC bound to Sla2p regulates other early cortical patch factors that interact with Sla2p to mediate a conformational change, or LC binding leads to their recruitment, which is required to drive progression of vesicle formation. Further studies will be required to distinguish among these models.

ACKNOWLEDGMENTS

We thank Mike Yaffe, Erin O'Shea, and Greg Payne for their gifts of many strains, plasmids, and antibodies. We thank Kenneth Henry, John Collette, and Ji Suk Chang for their helpful comments. T.M.N. was supported by National Institutes of Health (NIH) training grant T32 GM08056-20, and F.I. is a Ramon y Cajal postdoctoral fellow supported by Spain's Ministry of Education and Science. This work was funded by NIH Grant R01 GM55796 (S.K.L.) and Ministerio de Ciencia y Technologia Grants SAF2002-04707 and BUF2005-04089 (M.G.).

REFERENCES

Baggett, J. J., D'Aquino, K. E., and Wendland, B. (2003). The Sla2p talin domain plays a role in endocytosis in *Saccharomyces cerevisiae*. Genetics *165*, 1661–1674.

Brodsky, F. M., Chen, C. Y., Knuehl, C., Towler, M. C., and Wakeham, D. E. (2001). Biological basket weaving: formation and function of clathrin-coated vesicles. Annu. Rev. Cell. Dev. Biol. *17*, 517–568.

Chen, C. Y., and Brodsky, F. M. (2005). Huntingtin-interacting protein 1 (Hip1) and Hip1-related protein (Hip1R) bind the conserved sequence of clathrin light chains and thereby influence clathrin assembly in vitro and actin distribution in vivo. J. Biol. Chem. *280*, 6109–6117.

Chen, C. Y., Reese, M. L., Hwang, P. K., Ota, N., Agard, D., and Brodsky, F. M. (2002). Clathrin light and heavy chain interface: alpha-helix binding superhelix loops via critical tryptophans. EMBO J. *21*, 6072–6082.

Chu, D. S., Pishvaee, B., and Payne, G. S. (1996). The light chain subunit is required for clathrin function in *Saccharomyces cerevisiae*. J. Biol. Chem. *271*, 33123–33130.

Dulic, V., Egerton, M., Elguindi, I., Raths, S., Singer, B., and Riezman, H. (1991). Yeast endocytosis assays. Methods Enzymol. *194*, 697–710.

Engqvist-Goldstein, A. E., Kessels, M. M., Chopra, V. S., Hayden, M. R., and Drubin, D. G. (1999). An actin-binding protein of the Sla2/Huntingtin interacting protein 1 family is a novel component of clathrin-coated pits and vesicles. J. Cell Biol. *147*, 1503–1518.

Engqvist-Goldstein, A. E., Warren, R. A., Kessels, M. M., Keen, J. H., Heuser, J., and Drubin, D. G. (2001). The actin-binding protein Hip1R associates with clathrin during early stages of endocytosis and promotes clathrin assembly in vitro. J. Cell Biol. *154*, 1209–1223.

Fotin, A., Cheng, Y., Sliz, P., Grigorieff, N., Harrison, S. C., Kirchhausen, T., and Walz, T. (2004). Molecular model for a complete clathrin lattice from electron cryomicroscopy. Nature *432*, 573–579.

Henry, K. R., D'Hondt, K., Chang, J., Newpher, T., Huang, K., Hudson, R. T., Riezman, H., and Lemmon, S. K. (2002). Scd5p and clathrin function are important for cortical actin organization, endocytosis, and localization of Sla2p in yeast. Mol. Biol. Cell *13*, 2607–2625.

Huang, K. M., Gullberg, L., Nelson, K. K., Stefan, C. J., Blumer, K., and Lemmon, S. K. (1997). Novel functions of clathrin light chains: clathrin heavy chain trimerization is defective in light chain-deficient yeast. J. Cell Sci. *110* (Pt 7), 899–910.

Hyun, T. S., Rao, D. S., Saint-Dic, D., Michael, L. E., Kumar, P. D., Bradley, S. V., Mizukami, I. F., Oravecz-Wilson, K. I., and Ross, T. S. (2004). H.IP1 and H.IP1r stabilize receptor tyrosine kinases and bind 3-phosphoinositides via epsin N-terminal homology domains. J. Biol. Chem. *279*, 14294–14306.

Kaksonen, M., Sun, Y., and Drubin, D. G. (2003). A pathway for association of receptors, adaptors, and actin during endocytic internalization. Cell *115*, 475–487.

Kaksonen, M., Toret, C. P., and Drubin, D. G. (2005). A modular design for the clathrin- and actin-mediated endocytosis machinery. Cell *123*, 305–320.

Kaksonen, M., Toret, C. P., and Drubin, D. G. (2006). Harnessing actin dynamics for clathrin-mediated endocytosis. Nat. Rev. Mol. Cell Biol. *7*, 404–414.

Legendre-Guillemin, V., Metzler, M., Charbonneau, M., Gan, L., Chopra, V., Philie, J., Hayden, M. R., and McPherson, P. S. (2002). HIP1 and HIP12 display differential binding to F-actin, AP2, and clathrin. Identification of a novel interaction with clathrin light chain. J. Biol. Chem. *277*, 19897–19904.

Legendre-Guillemin, V., Metzler, M., Lemaire, J. F., Philie, J., Gan, L., Hayden, M. R., and McPherson, P. S. (2005). Huntingtin interacting protein 1 (HIP1) regulates clathrin assembly through direct binding to the regulatory region of the clathrin light chain. J. Biol. Chem. *280*, 6101–6108.

Lemmon, S., Lemmon, V. P., and Jones, E. W. (1988). Characterization of yeast clathrin and anticlathrin heavy-chain monoclonal antibodies. J. Cell. Biochem. *36*, 329–340.

Lemmon, S. K., and Jones, E. W. (1987). Clathrin requirement for normal growth of yeast. Science *238*, 504–509.

Liu, S. H., Wong, M. L., Craik, C. S., and Brodsky, F. M. (1995). Regulation of clathrin assembly and trimerization defined using recombinant triskelion hubs. Cell *83*, 257–267.

Longtine, M. S., McKenzie, A., 3rd, Demarini, D. J., Shah, N. G., Wach, A., Brachat, A., Philippsen, P., and Pringle, J. R. (1998). Additional modules for versatile and economical PCR-based gene deletion and modification in *Saccharomyces cerevisiae*. Yeast *14*, 953–961.

McCann, R. O., and Craig, S. W. (1997). The I/LWEQ module: a conserved sequence that signifies F-actin binding in functionally diverse proteins from yeast to mammals. Proc. Natl. Acad. Sci. USA *94*, 5679–5684.

Nelson, K. K., and Lemmon, S. K. (1993). Suppressors of clathrin deficiency: overexpression of ubiquitin rescues lethal strains of clathrin-deficient *Saccharomyces cerevisiae*. Mol. Cell. Biol. *13*, 521–532.

Newpher, T. M., and Lemmon, S. K. (2006). Clathrin is important for normal actin dynamics and progression of Sla2p-containing patches during endocytosis in yeast. Traffic *7*, 574–588.

Newpher, T. M., Smith, R. P., Lemmon, V., and Lemmon, S. K. (2005). In vivo dynamics of clathrin and its adaptor-dependent recruitment to the actin-based endocytic machinery in yeast. Dev. Cell *9*, 87–98.

Payne, G. S., and Schekman, R. (1989). Clathrin: a role in the intracellular retention of a Golgi membrane protein. Science *245*, 1358–1365.

Scarmato, P., and Kirchhausen, T. (1990). Analysis of clathrin light chain-heavy chain interactions using truncated mutants of rat liver light chain LCB3. J. Biol. Chem. *265*, 3661–3668.

Senetar, M. A., Foster, S. J., and McCann, R. O. (2004). Intrasteric inhibition mediates the interaction of the I/LWEQ module proteins Talin1, Talin2, Hip1, and Hip12 with actin. Biochemistry *43*, 15418–15428.

Sun, Y., Kaksonen, M., Madden, D. T., Schekman, R., and Drubin, D. G. (2005). Interaction of Sla2p's ANTH domain with PtdIns(4,5)P2 is important for actin-dependent endocytic internalization. Mol. Biol. Cell *16*, 717–730.

Toshima, J. Y., Toshima, J., Kaksonen, M., Martin, A. C., King, D. S., and Drubin, D. G. (2006). Spatial dynamics of receptor-mediated endocytic trafficking in budding yeast revealed by using fluorescent alpha-factor derivatives. Proc. Natl. Acad. Sci. USA *103*, 5793–5798.

Ungewickell, E., and Ungewickell, H. (1991). Bovine brain clathrin light chains impede heavy chain assembly in vitro. J. Biol. Chem. *266*, 12710–12714.

Yang, S., Cope, M. J., and Drubin, D. G. (1999). Sla2p is associated with the yeast cortical actin cytoskeleton via redundant localization signals. Mol. Biol. Cell *10*, 2265–2283.

Ybe, J. A., Greene, B., Liu, S. H., Pley, U., Parham, P., and Brodsky, F. M. (1998). Clathrin self-assembly is regulated by three light-chain residues controlling the formation of critical salt bridges. EMBO J. *17*, 1297–1303.